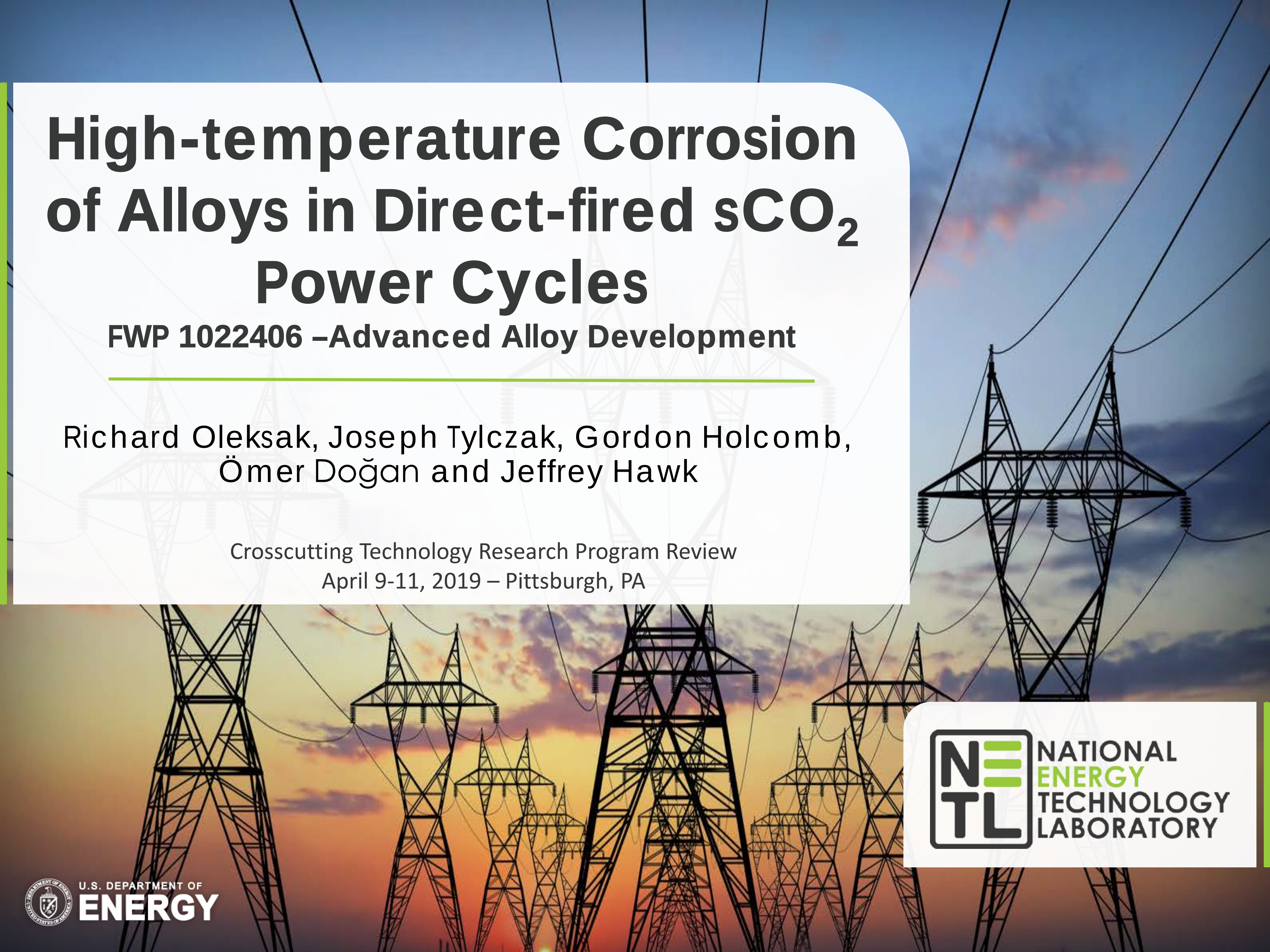

High-temperature Corrosion of Alloys in Direct-fired sCO_2 Power Cycles

FWP 1022406 –Advanced Alloy Development

Richard Oleksak, Joseph Tylczak, Gordon Holcomb,
Ömer Doğan and Jeffrey Hawk

Crosscutting Technology Research Program Review
April 9-11, 2019 – Pittsburgh, PA

NATIONAL ENERGY TECHNOLOGY LABORATORY

U.S. DEPARTMENT OF ENERGY

Acknowledgements

This work was performed in support of the US Department of Energy's Fossil Energy Crosscutting Technology Research Program, Regis Conrad (FE HQ Program Manager) and Briggs White (NETL Crosscutting Technology Manager). The Research was executed through NETL Research and Innovation Center's Advanced Alloy Development Field Work Proposal (Bryan Morreale, Director). Research performed by Leidos Research Support Team was conducted under the RSS contract 89243318CFE000003.

DISCLAIMER

Direct-fired sCO_2 Power Cycles

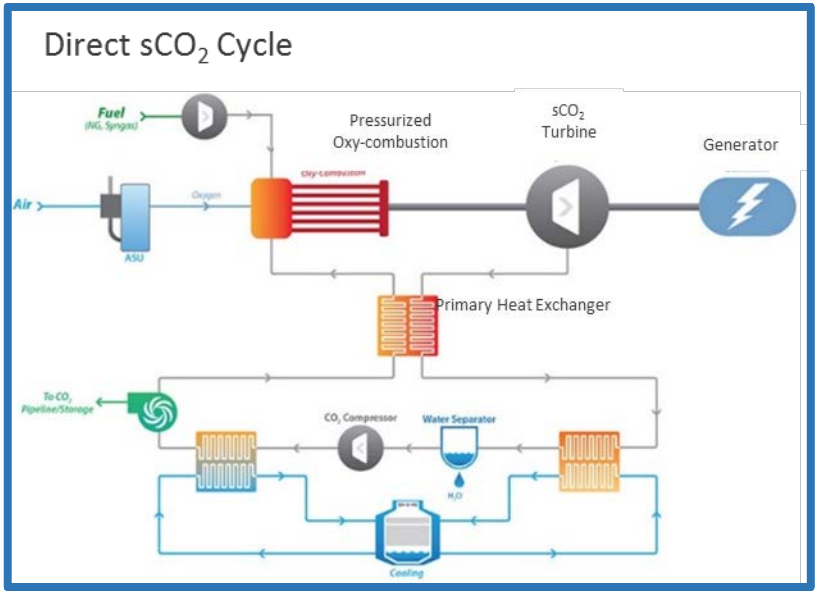
Direct sCO_2 Cycle

Higher Efficiency

- High working fluid temperatures
- Recompression near liquid densities
- High heat recuperation

Lower Capital Cost

- Compact turbo machinery
- Simple configurations

Lower Environmental Impact

- Zero emissions
- Dry cooling
- Water production

Materials Issues

Allam Cycle

Typical working fluid

CO_2 – 95%

H_2O - 4%

O_2 - 1%

Direct sCO_2 Cycle

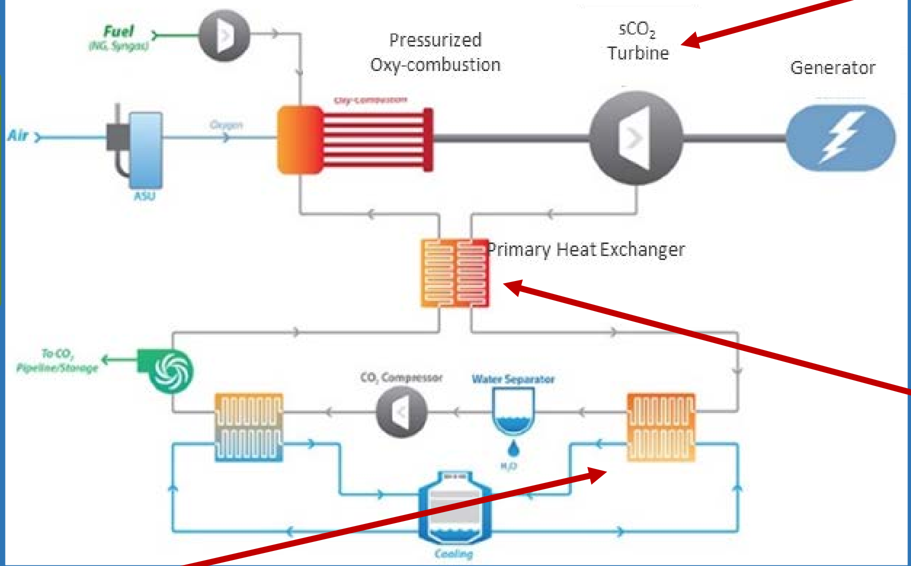

Turbine

- Oxidation
- Creep-fatigue in sCO_2
- Erosion

PHX

- High cost
- Difficult to join alloys
- Carburization of Fe-based alloys
- High-temperature oxidation of alloys
- Corrosion due to $H2_SO_4$ condensation
- Creep-fatigue in sCO_2

Recuperator

- High cost
- Carburization of Fe-based alloys
- Corrosion due to carbonic acid condensation
- Corrosion due to sulfuric acid condensation

Candidate Alloys

Several commercially available structural alloys were tested*:

wt%	Fe	Ni	Cr	Co	Mo	Mn	W	Nb	Si	Ti	Al	C
Iron-based (ferritic)												
GR 22	96	0.15	**2.29**	--	0.94	0.52	--	0.00	0.21	0.00	0.03	0.13
GR 91	90	0.09	**8.37**	--	0.90	0.45	--	0.07	0.33	0.00	0.01	0.09
Iron-based (austenitic/ferritic stainless)												
347H	70.13	9.01	**17.34**	0.14	0.37	1.86	--	0.52	0.31	0.00	--	0.05
304H	70.63	8.27	**18.74**	0.22	0.12	1.08	0.01	0.01	0.44	0.00	0.01	
310	54	19.10	**25.04**	0.17	0.09	1.39	--	0.01	0.39	0.00	0.02	0.04
E-Brite	71.64	0.21	**26.50**	0.02	1.00	0.04	<0.010	0.12	0.25	<0.001	0.10	--
Nickel-based (solution strengthened)												
600	7.58	74.97	**16.01**	0.07	0.23	0.22	<0.010	0.11	0.15	0.33	0.14	--
617	0.39	55.07	**21.89**	11.45	9.61	0.04	<0.010	0.03	0.02	0.47	0.91	--
230	0.40	59.79	**22.21**	0.34	1.26	0.51	14.39	0.04	0.44	0.01	0.42	--
625	4.44	60	**22.32**	0.03	8.33	0.36	--	3.50	0.23	0.19	0.14	0.08
Nickel-based (precipitation strengthened)												
718	18.14	53.81	**17.97**	0.16	3.03	0.24	--	5.30	0.08	1.02	1.55	0.05
282	0.15	58.20	**19.34**	12.12	8.44	0.08	--	0.02	0.17	2.13	1.29	--
263	0.42	50.70	**20.31**	19.65	5.84	0.35	--	0.08	0.02	2.18	0.39	0.06
740H	<0.010	50.43	**24.54**	20.22	0.31	0.24	<0.010	1.53	0.12	1.38	1.20	--

Increasing Cr content

*Also some preliminary results for additional 9Cr steels (CPJ7N, JMP3, JMP4, SAVE 12B) and intermediate Cr (11.5-16.7 wt%) 400 series steels

High Temperature Oxidation Exposures

Gas 1 (vol%): 95% CO_2, 4% H_2O, 1% O_2

Gas 2 (vol%): 95% CO_2, 4% H_2O, 1% O_2, 0.1% SO_2

Pressure: 1 atm

Temperature: Ni alloys: 750°C
(tests underway at 600, 650, 700, 800°C)

Fe alloys: 550, 600, 650°C

Duration: 2500 h (500 h increments)

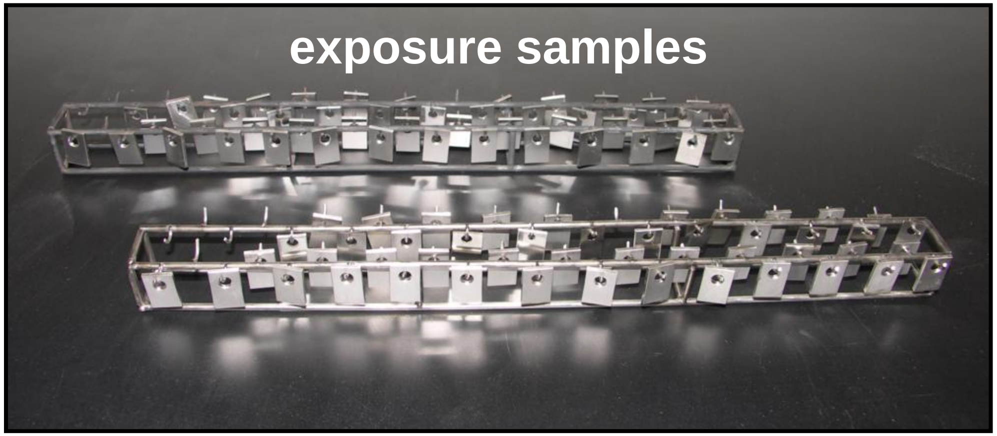
exposure samples

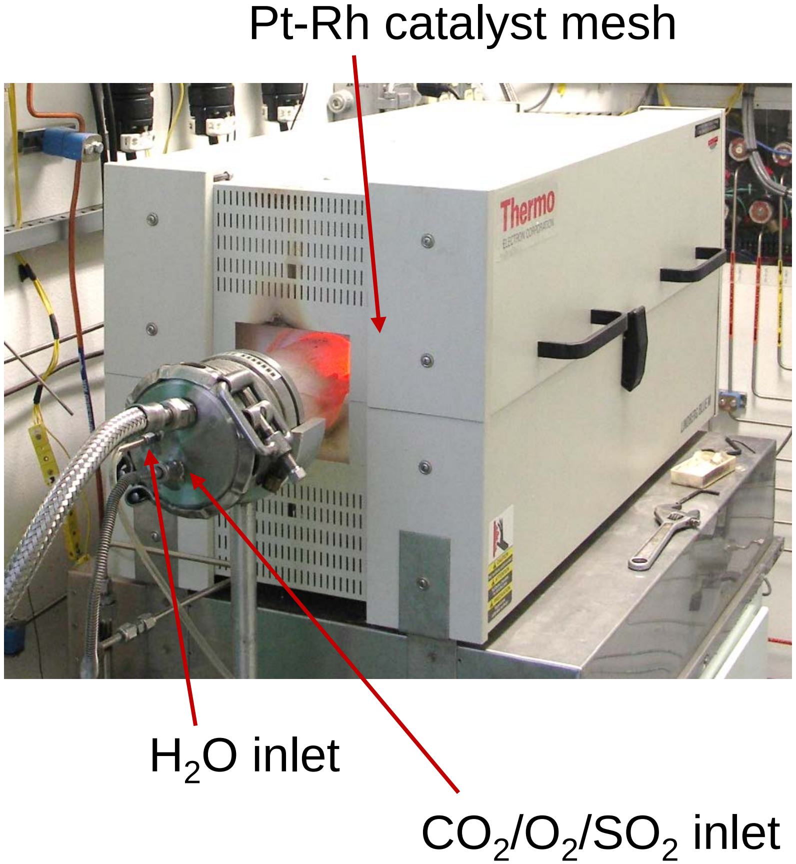

Direct sCO_2 Power Cycle Environments

Alloy Performance

- **Objective:** Identify alloys with sufficient corrosion resistance and strength for use as heat exchangers in high-efficiency fossil fuel-fired direct sCO_2 power cycles.
- **Challenges:** Very limited alloy performance data are available to be used in the manufacture of recuperators, or to validate the predictive models, for direct-fired sCO_2 power cycles.
- **Benefit:** Generate materials performance data relevant to the direct-fired sCO_2 power cycles, and identify materials which can be used to reduce risk in commercialization of the technology.
- **Approach:** Power plant materials, including A-USC alloys, will be exposed to conditions simulating environments found in the high-temperature components of direct-fired sCO_2 power cycles to determine:
  - Parabolic rate constants for determining long-term oxide scale thickness and to validate the predictive models for oxidation scale growth and exfoliation;
  - Effect of impurities (i.e., O_2, H_2O, and SO_2 in CO_2) on the high-temperature oxidation of structural materials; and
  - Effect of the direct sCO_2 cycle environment on creep, fatigue, & creep-fatigue behavior.

9Cr Fe alloys (and P22)

Mass change without and with SO_2

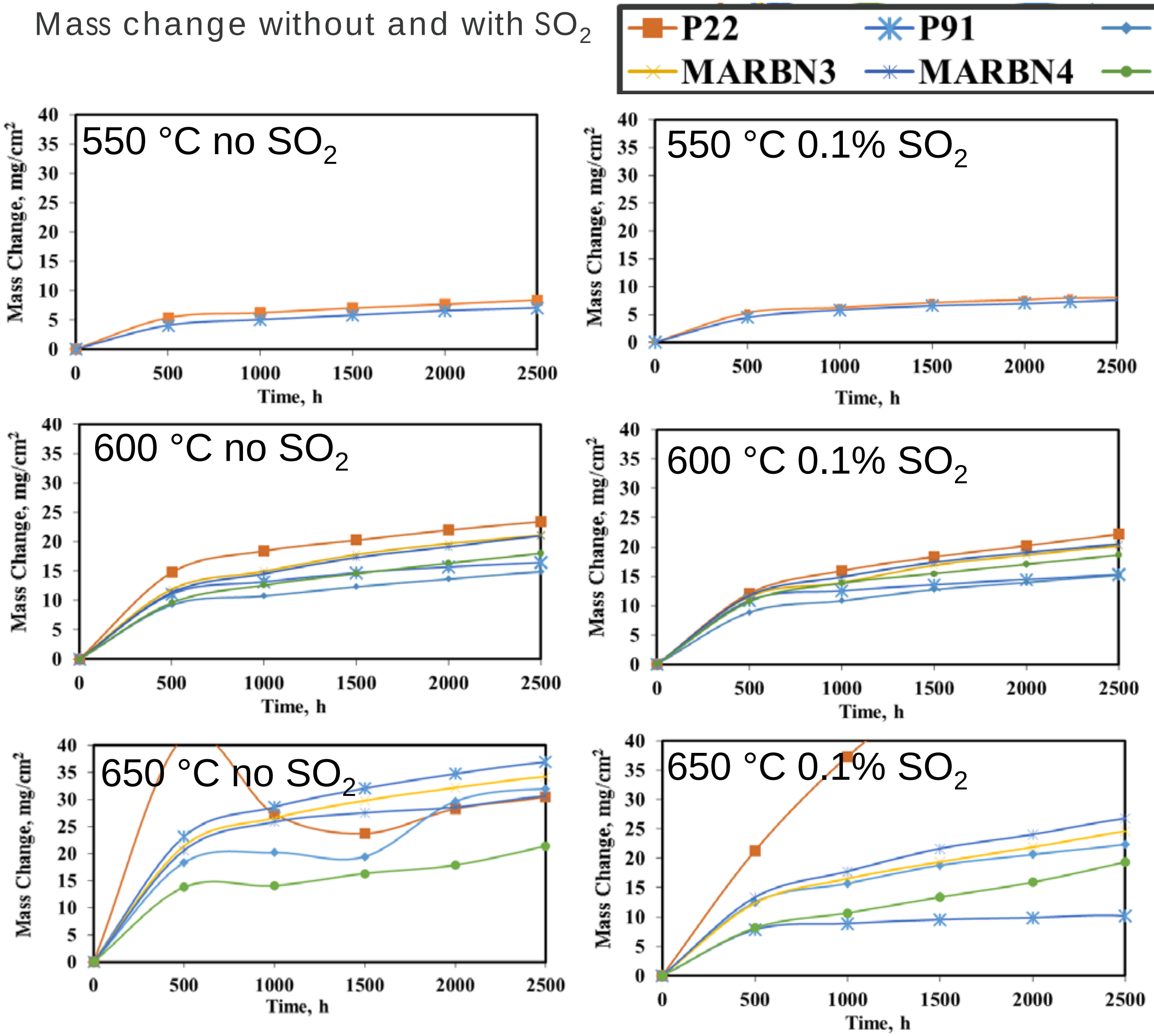

- All 9Cr (and P22) Fe steels show similar & high oxidation rates, which increase with temperature.
- SO_2 has minimal effect, potentially even beneficial at higher temperatures.

High-Cr (>17 wt%) Fe alloys

Mass change without and with SO$_2$

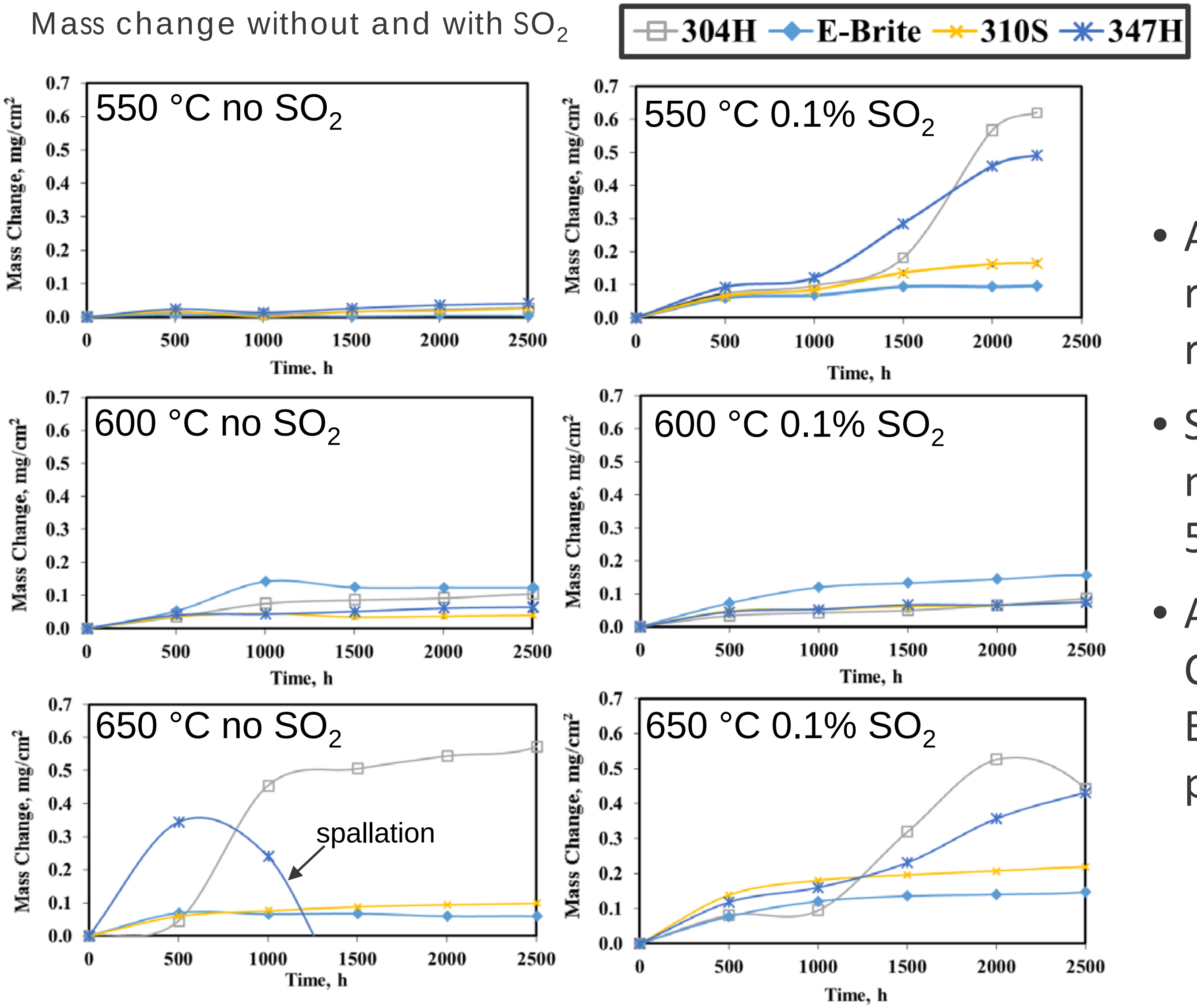

- All high-Cr alloys show relatively low oxidation rates.
- SO$_2$ has a strong negative effect at 550°C.
- Alloys with the highest Cr content (310S, E-Brite) generally perform the best.

Comparing temperatures for Fe alloys

Mass change plots for a typical 9Cr (left) and high-Cr (right) Fe alloy

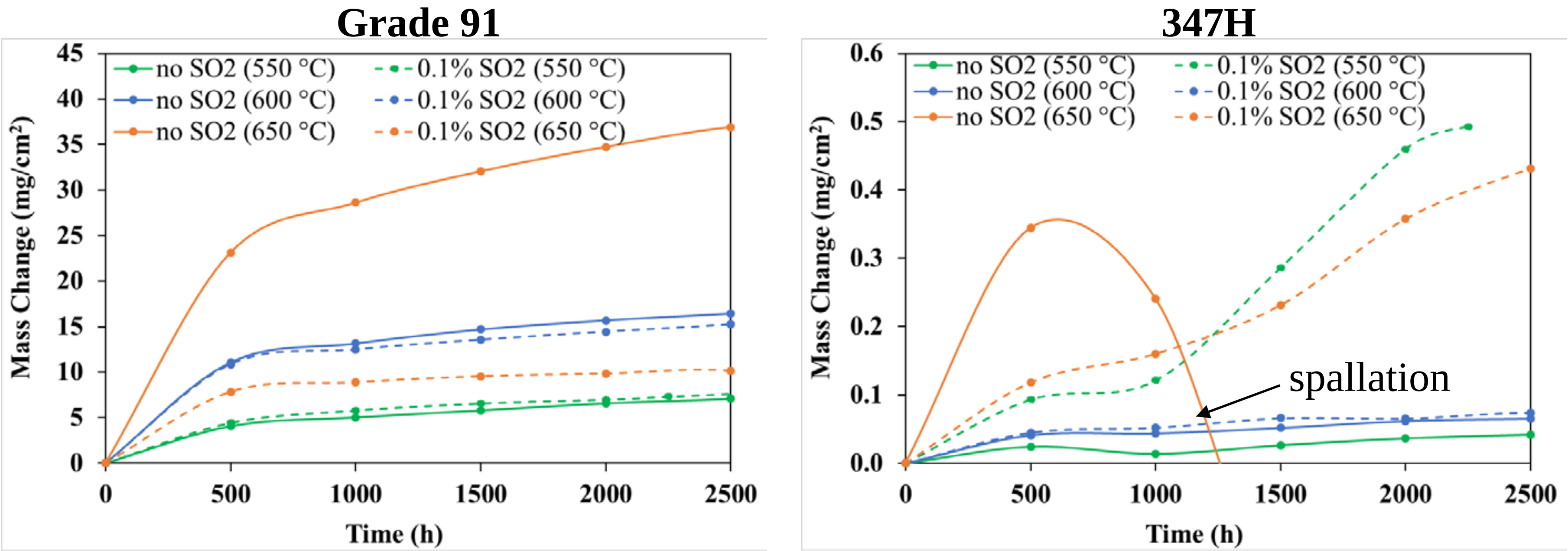

Grade 91

347H

- The 9Cr (and lower Cr) steels show high oxidation rates that generally increase with temperature. For these alloys SO_2 has minimal effect at 550 and 600°C & is beneficial at 650°C.
- The high-Cr steels show much lower oxidation rates & a complex pattern of behavior with SO_2. At 550°C it is detrimental, 600°C it has minimal effect, & 650°C is potentially beneficial by preventing spallation.

Analysis of 9Cr Fe alloys (550 °C)

SEM imaging of Grade 91 exposed without and with SO_2

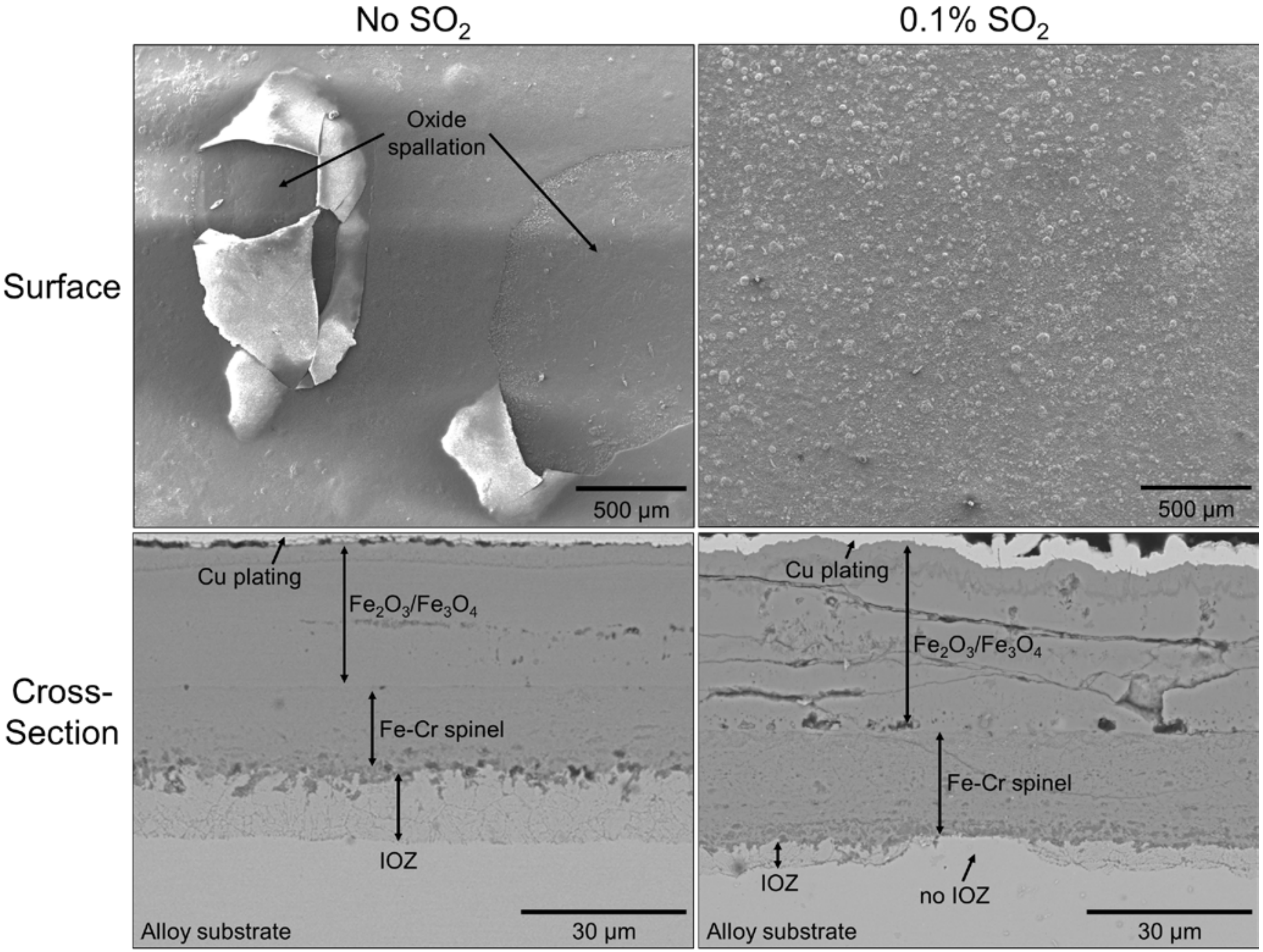

- Thick Fe-rich oxide scales.
- SO_2 is actually beneficial by reducing oxide spallation & internal oxidation.
- Slightly thicker oxide for exposure done with SO_2.

Analysis of 9Cr Fe alloys (550 °C)

X-ray mapping of Grade 91 exposed with SO_2

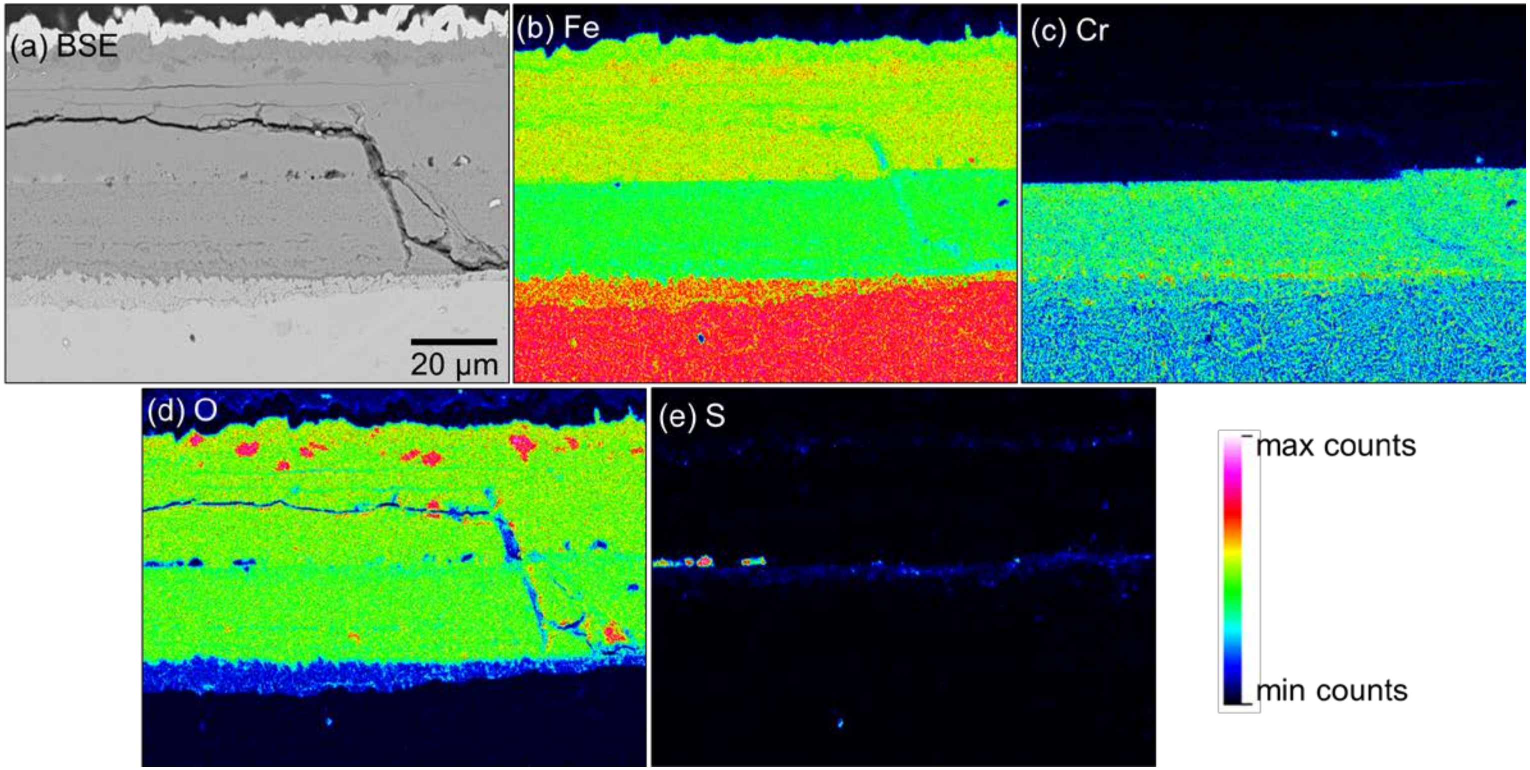

- Fe-rich duplex oxide scale, similar to what is observed during exposure to pure CO_2.
- Sulfides observed within the scale, preferentially at the inner/outer oxide layer interface.
- Presence of sulfides does not appear to significantly affect the oxidation in the case of thick Fe-rich oxide scales.

Analysis of 9Cr Fe alloys (550 °C)

SEM of Grade 91 after etching to assess for carburization

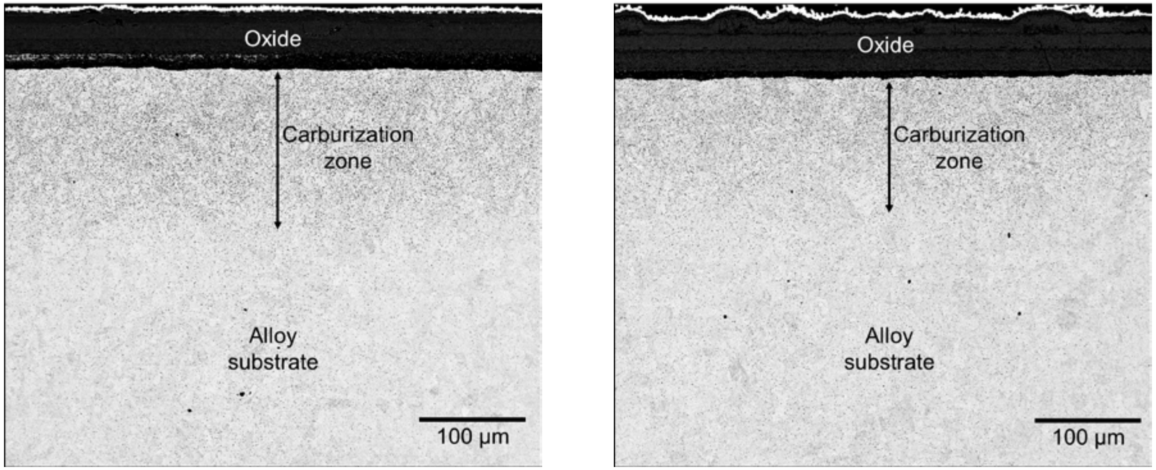

No SO_2

0.1% SO_2

Oxide/Alloy Interface

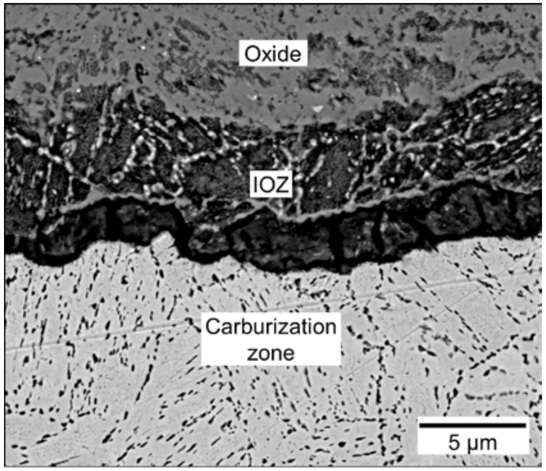

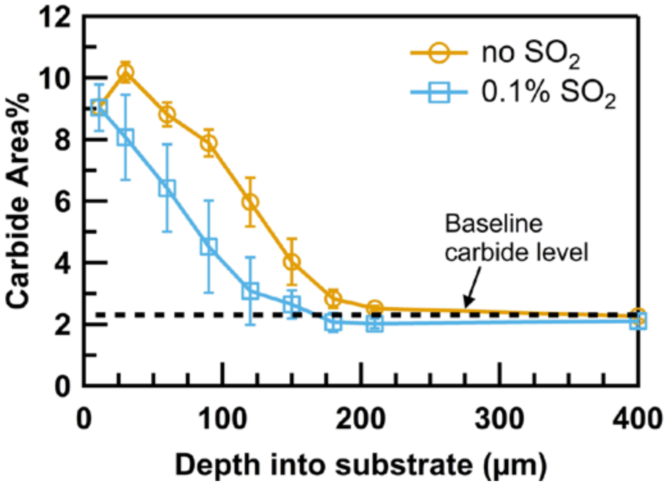

- Metal carbides form in the alloy to significant depths (100-200 µm) beneath Fe-rich oxide scales.
- The presence of SO_2 reduces internal carburization by competing with CO_2/CO for adsorption sites during oxidation.

Analysis of high-Cr Fe alloys (550 °C)

SEM imaging of 347H exposed without and with SO_2

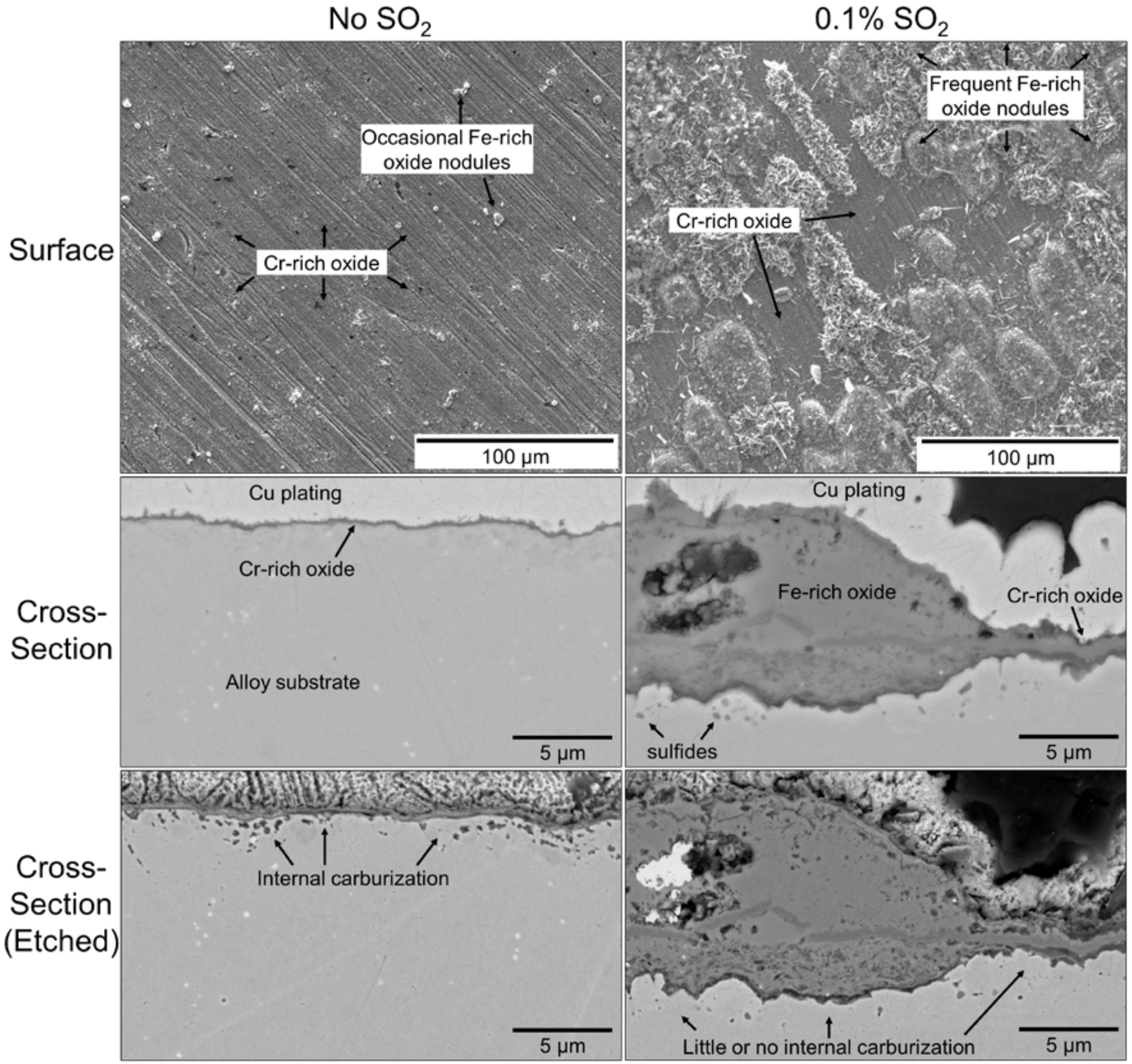

- Thin Cr-rich oxide scales formed during SO_2-free exposures.
- Addition of SO_2 caused breakdown leading to growth of Fe-rich oxide nodules.
- Shallow carburization occurred, which was reduced in the presence of SO_2.

Analysis of high-Cr Fe alloys (550 °C)

X-ray mapping of 347H exposed with SO_2

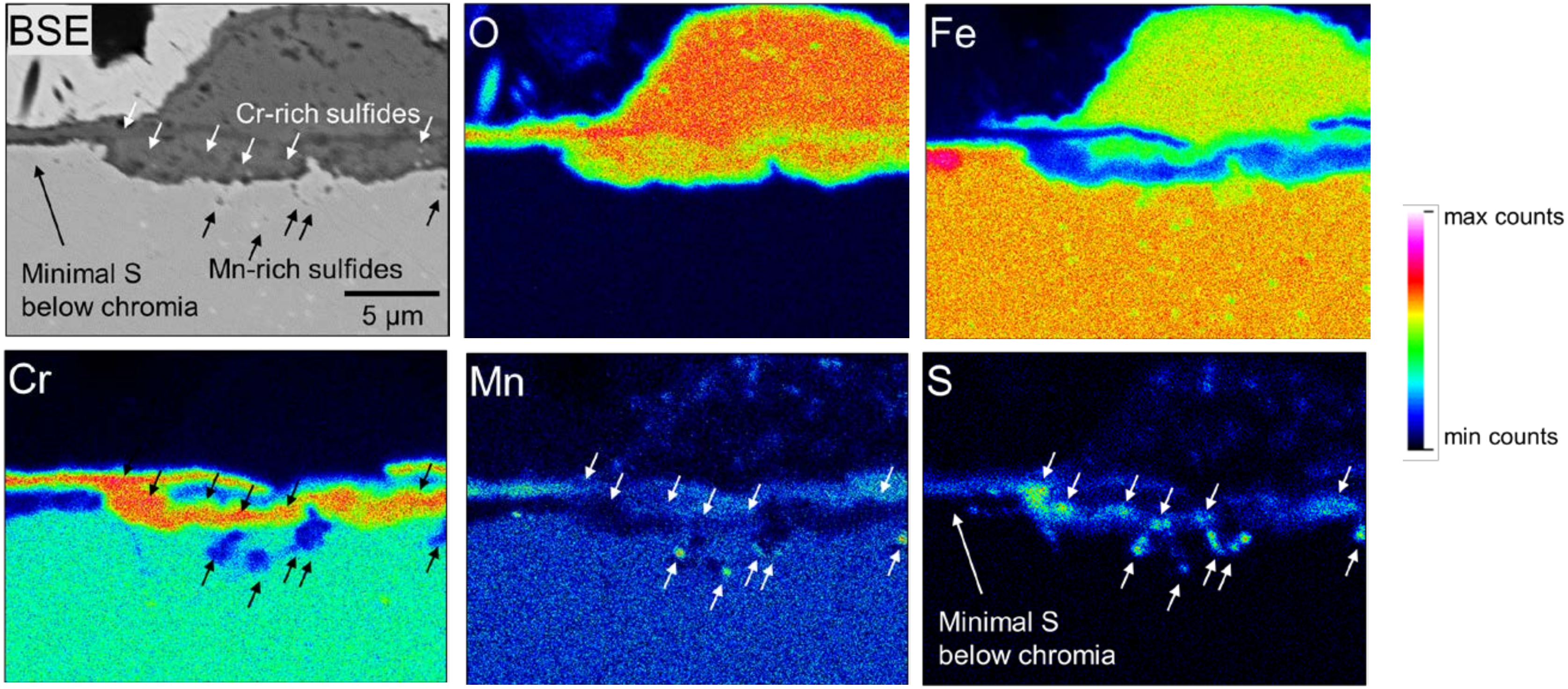

- Sulfides are observed within and below the oxide layer, which are correlated primarily with Mn & Cr.
- Significantly more sulfides are seen beneath the thick Fe-rich oxide nodules.

Mechanism of chromia breakdown in high-Cr Fe alloys at 550 °C

TEM analysis of 347H exposed with SO_2

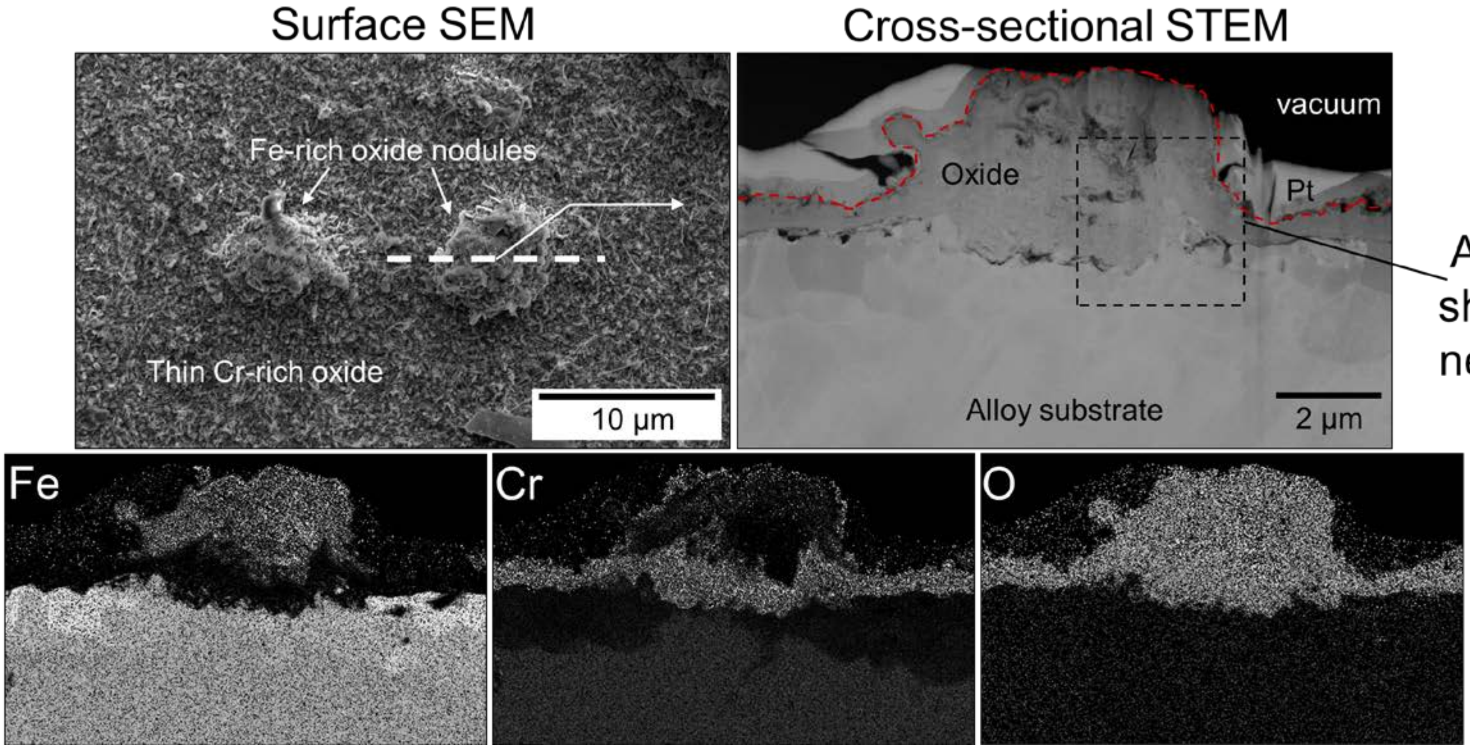

Analysis shown on next slide

- TEM was used to investigate the early stages of Fe-rich oxide nodule growth for exposures with SO_2.
- The cross-section captures an Fe-rich oxide nodule that has begun to grow above the thin Cr-rich oxide layer.

Mechanism of chromia breakdown in high-Cr Fe alloys at 550 °C

TEM analysis of 347H exposed with SO_2

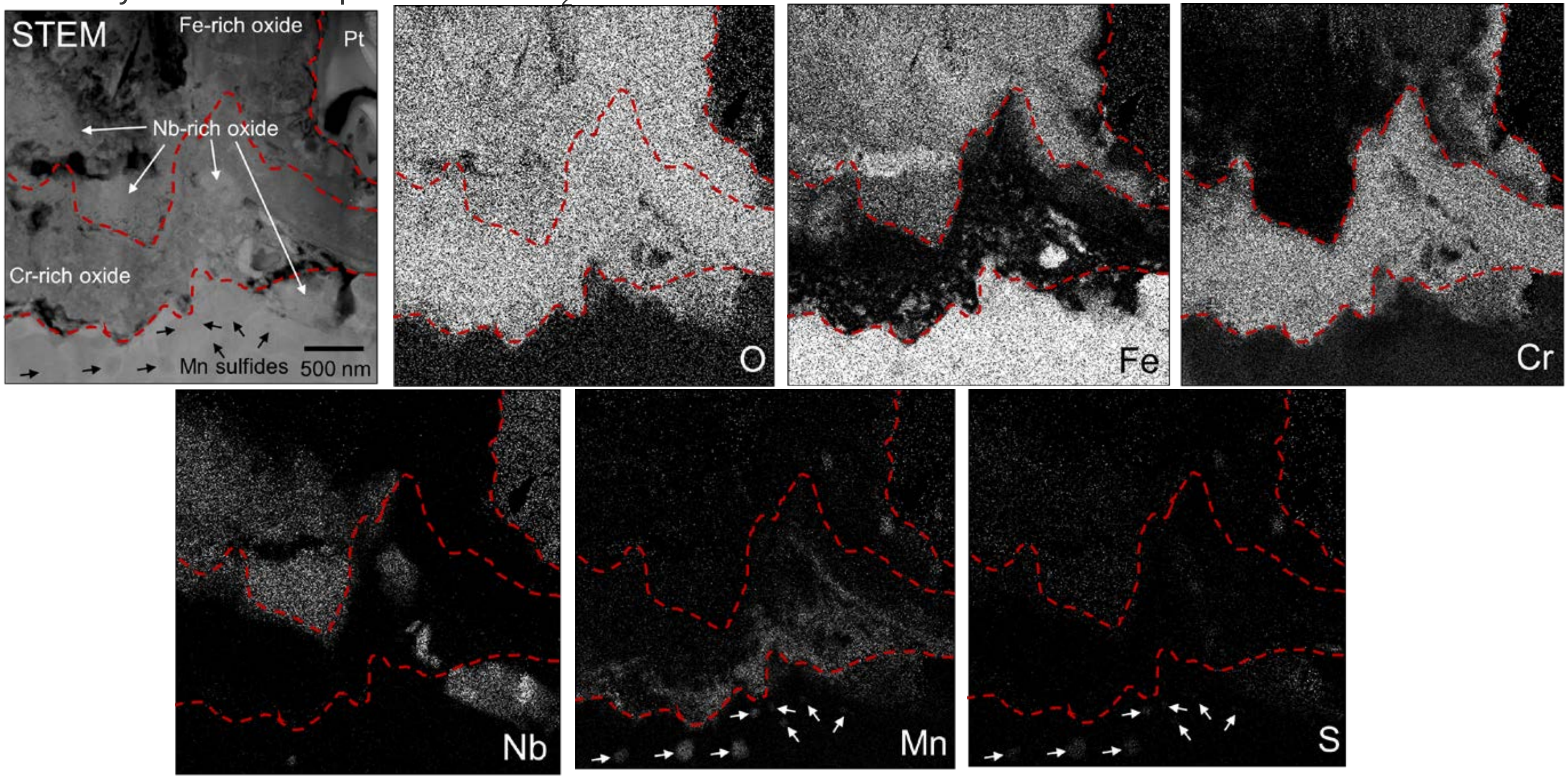

- Early stages of nodule formation are associated with significant Mn sulfide formation in the underlying alloy. This suggests a local increase in the permeability of SO_2 (or SO_3) that resulted in failure of the originally formed Cr-rich oxide scale.

Thermodynamic analysis of Fe alloys exposed with SO_2 (550 °C)

Diagrams showing stable compounds as a function of oxygen, sulfur, and carbon activity

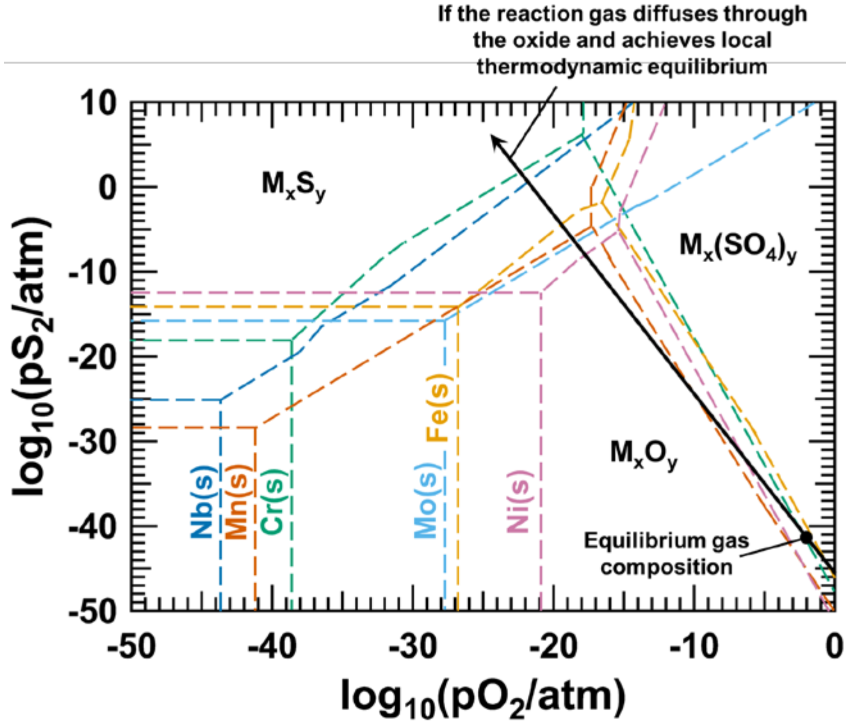

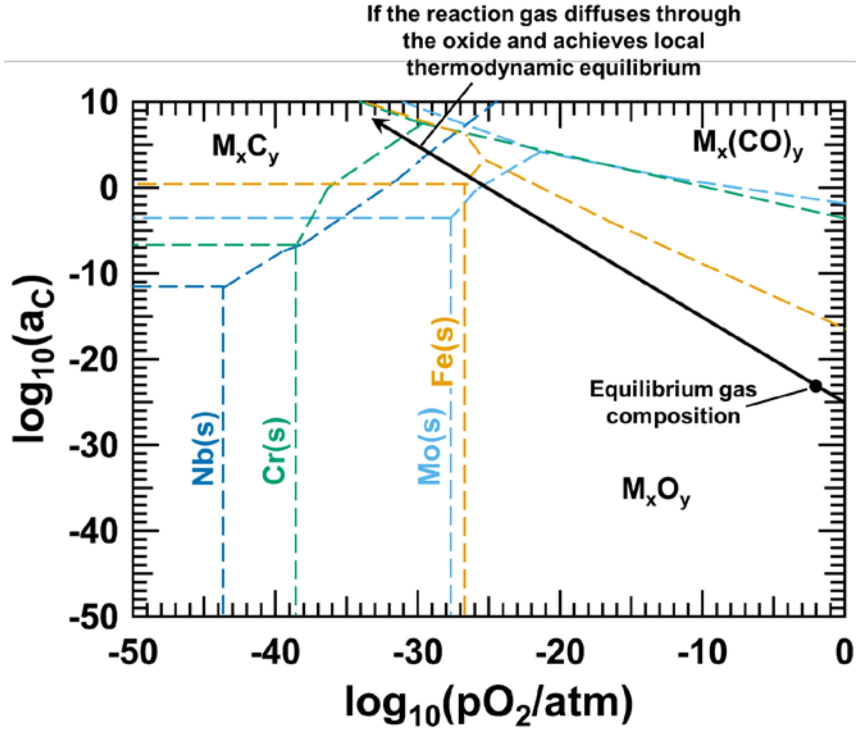

- Oxides are the stable compounds for most elements in equilibrium with the gas, however sulfates of Cr, Ni, and Mn can exist at the outermost surface.
- If the gas (SO_2, CO_2, etc.) successfully diffuses through & achieves local equilibrium with the oxide/underlying alloy, then formation of carbides & sulfides are predicted, consistent with the experimental observations.

Effect of Cr content on oxidation behavior of Fe alloys

Plots showing mass change at 1500h exposure time vs Cr content of the tested alloys

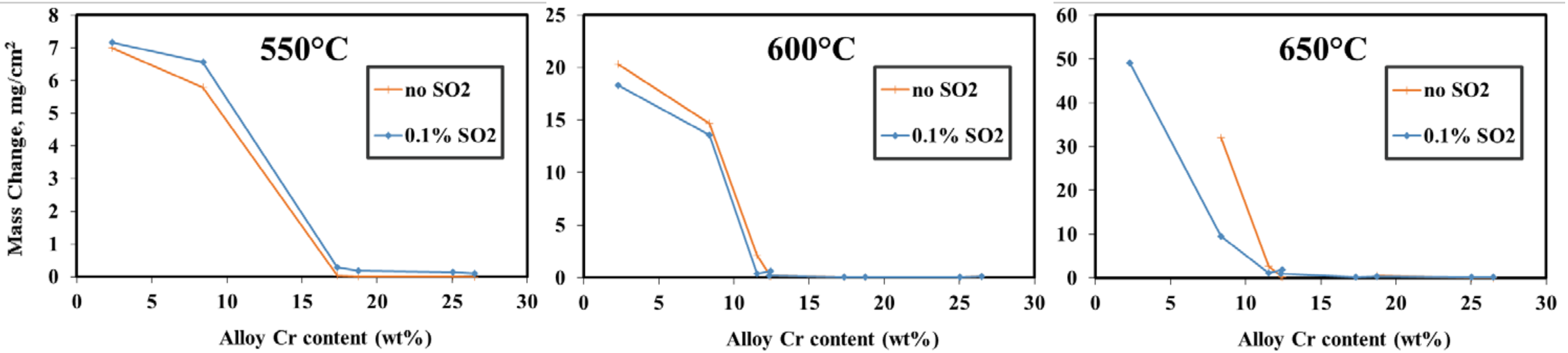

- There is a clear transition from Fe-rich oxides & high oxidation rates to Cr-rich oxides & low oxidation rates for Cr content above ≈11.5 wt%.
- Additional Cr beyond 11.5 wt% offers some additional benefit, particularly when SO_2 is present.

Ni alloys

Mass change without and with SO_2

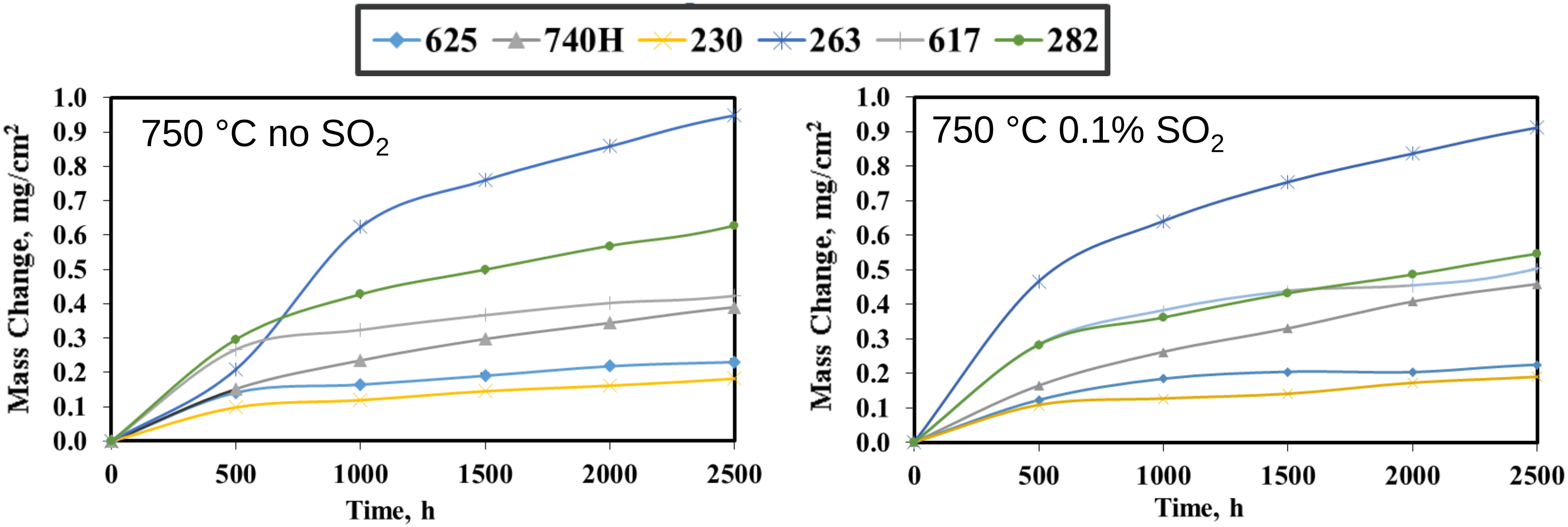

- Low mass gains and no effect of SO_2 for all Ni alloys at 750°C.
- Alloy 263 showed slightly higher mass gains than the other alloys.
- Preliminary results suggest negative effect of SO_2 at lower temperatures (more on this later).

Analysis of Ni alloys (750 °C)

SEM imaging of Ni alloys exposed with and without SO_2

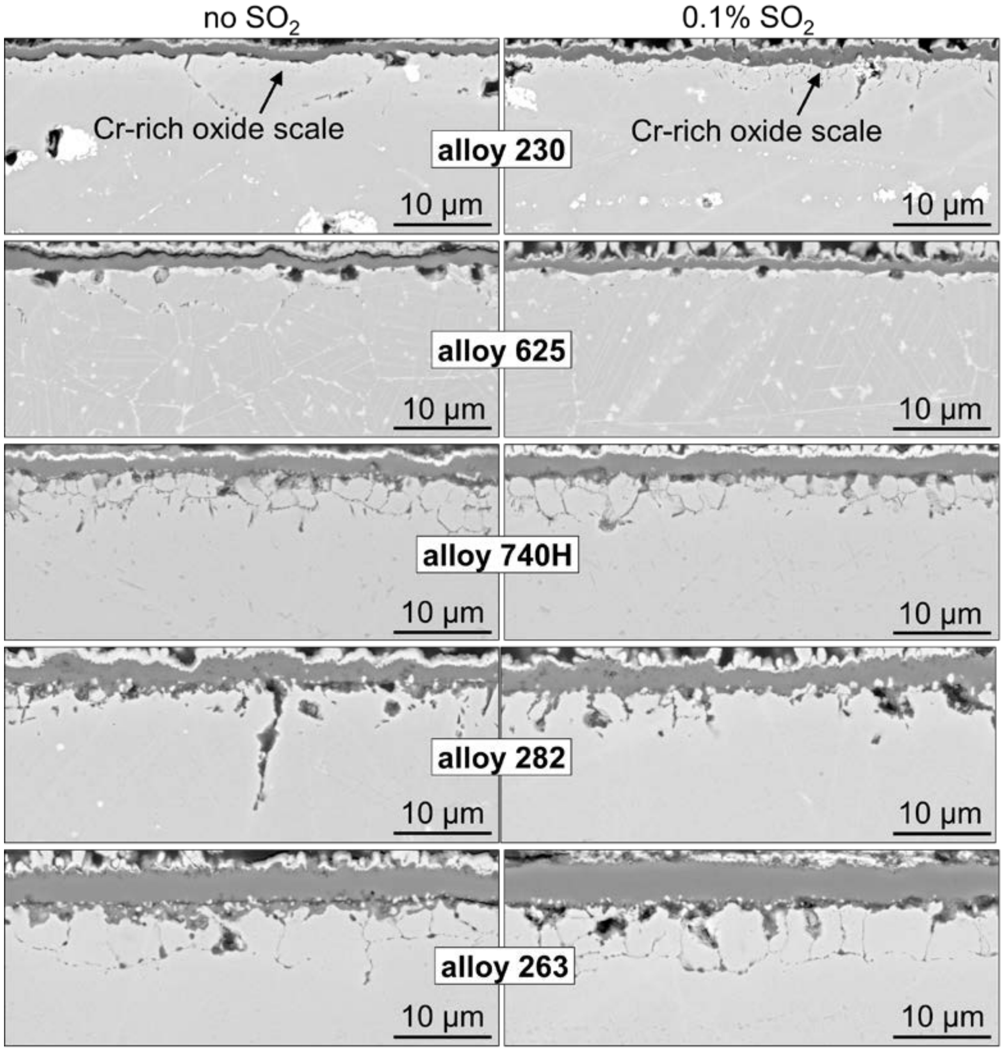

- Cross-sectional SEM shows that at 750 °C all Ni alloys formed thin Cr-rich oxide scales.
- A minor exception was observed for Alloy 263.
- No difference due to the addition of 0.1% SO_2.

Analysis of Alloy 263 (750 °C)

X-ray mapping of a region typical of most of the surface (no SO_2)

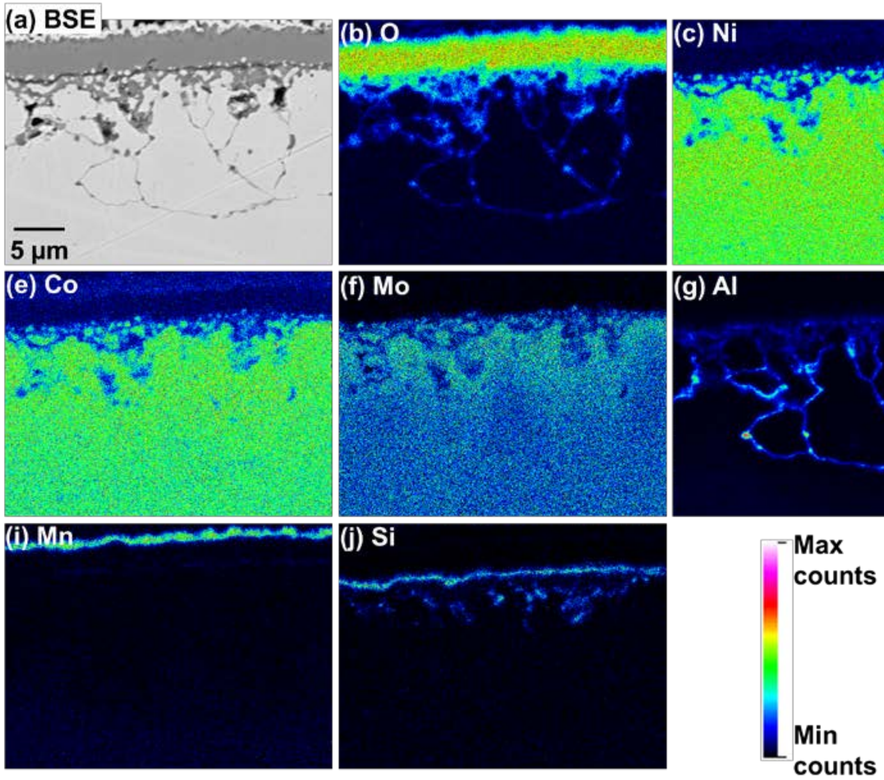

- Cr-rich oxide scale
- Internal oxidation of Al, Ti, Si
- Significant Ti-rich oxide also present at the surface of the scale

Analysis of Alloy 263 (750 °C)

X-ray mapping of a region of protective scale failure (no SO_2)

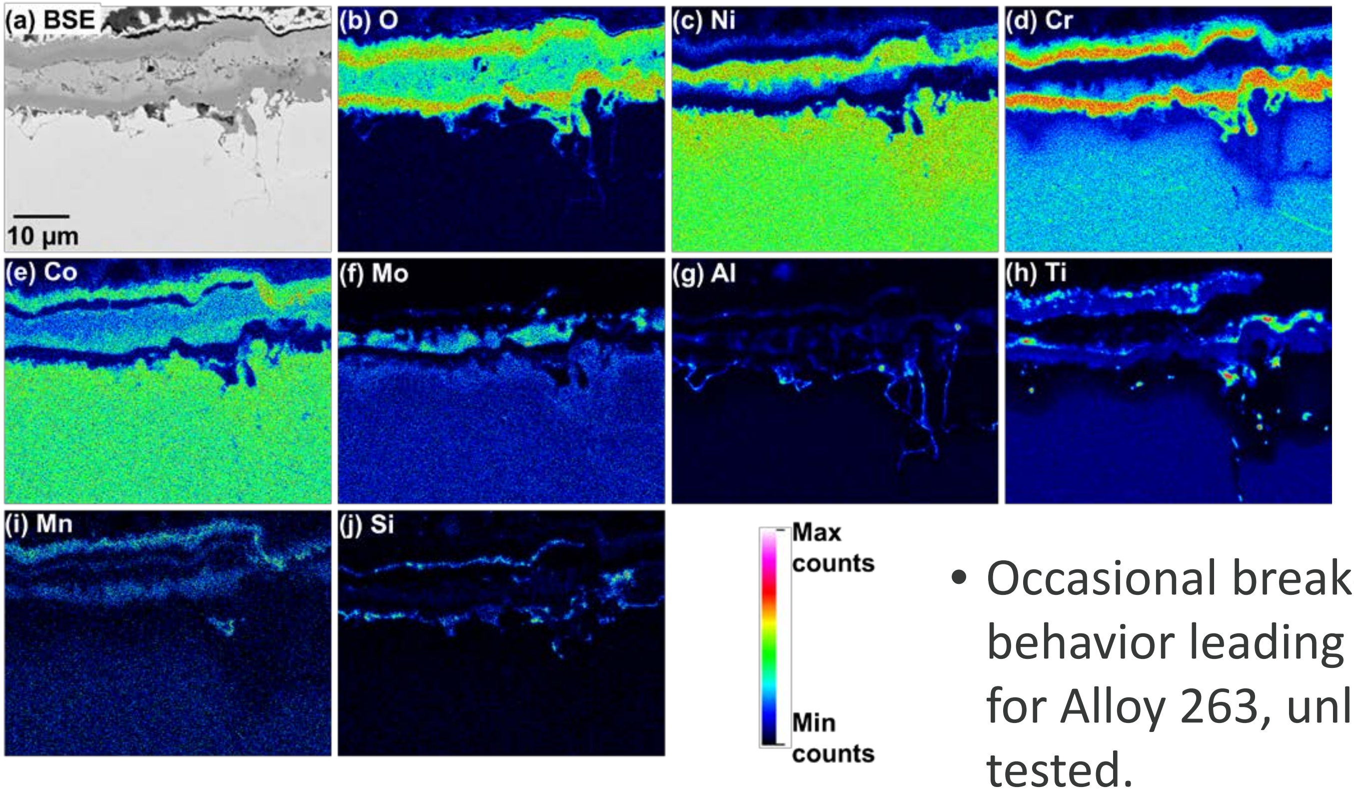

- Occasional breakdown in protective behavior leading to Ni-rich oxide nodules for Alloy 263, unlike for all other Ni alloys tested.
- This is thought to be related to an effect of minor alloy additions (next slide).

Effect of Ni alloy composition on oxidation rate (750 °C)

Plots showing mass change at 2500 h exposure time vs. composition of alloying elements of interest

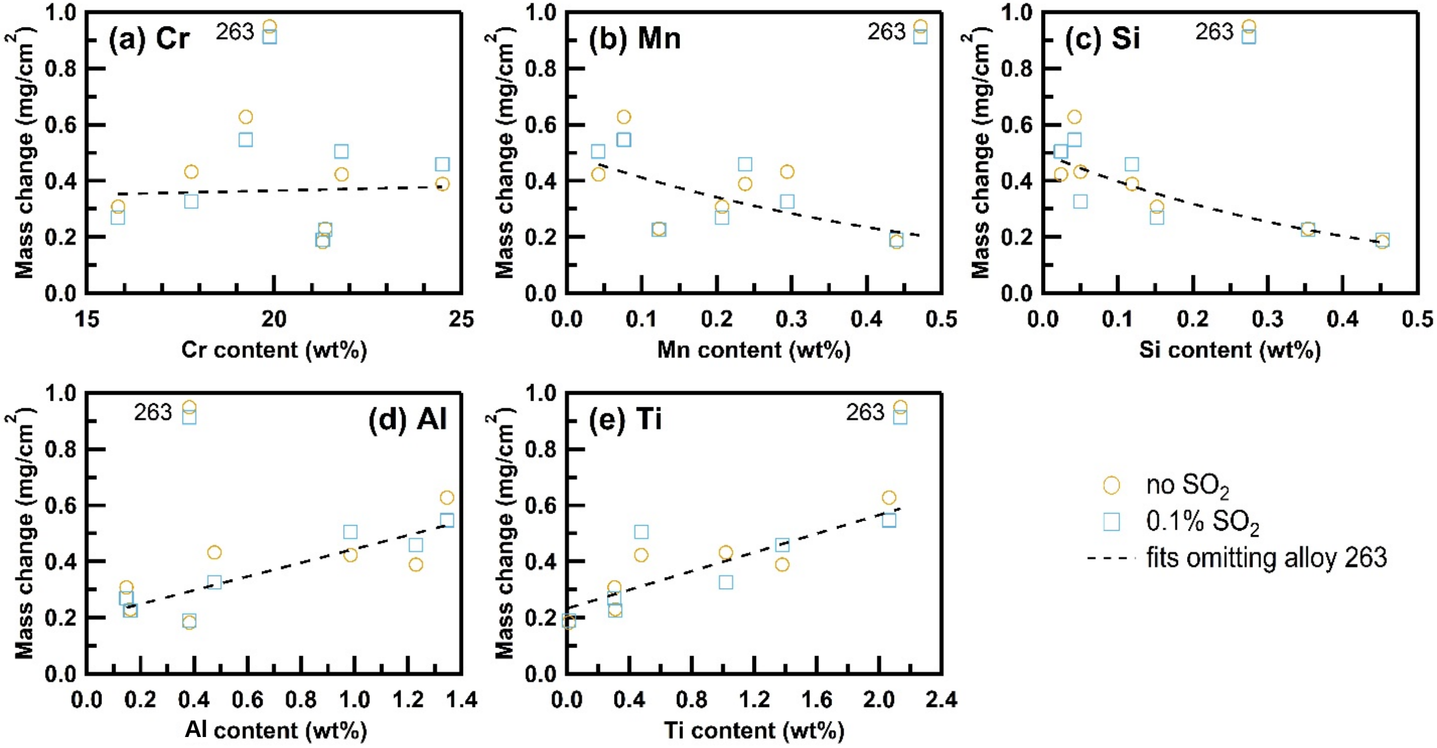

- Oxidation rate was not affected by Cr, decreased slightly with Mn & Si additions, and increased slightly with Al & Ti additions.
- The combination of high Ti & high Mn caused the highest oxidation rate (with occasional nodule growth) for Alloy 263.

Thermodynamic analysis of Ni alloys exposed with SO_2 (750 °C)

Diagrams showing stable compounds as a function of oxygen, sulfur, and carbon activity

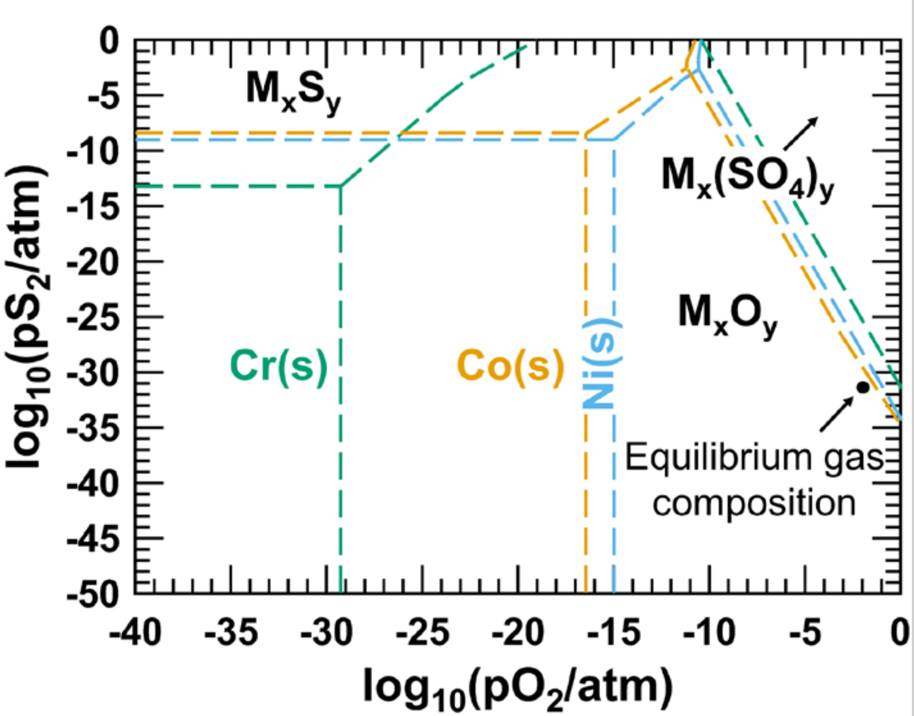

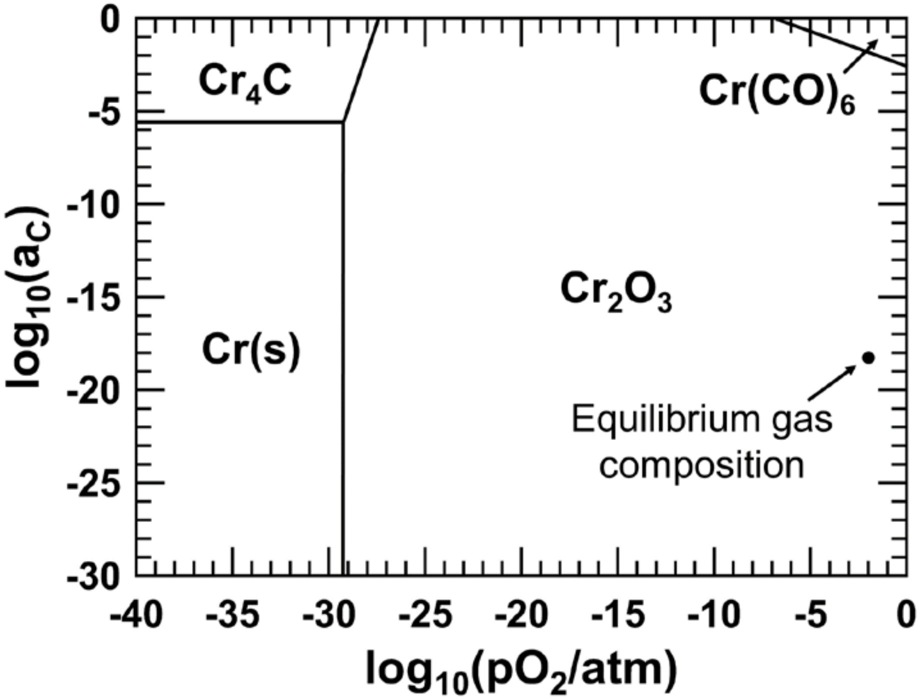

- Thermodynamic analysis shows that oxides are the stable compounds in equilibrium with the gas.
- General agreement with experimental results, where only oxides are observed.

Ni alloys

Mass change plots showing effect of temperature (left) and comparison to other environments (right)

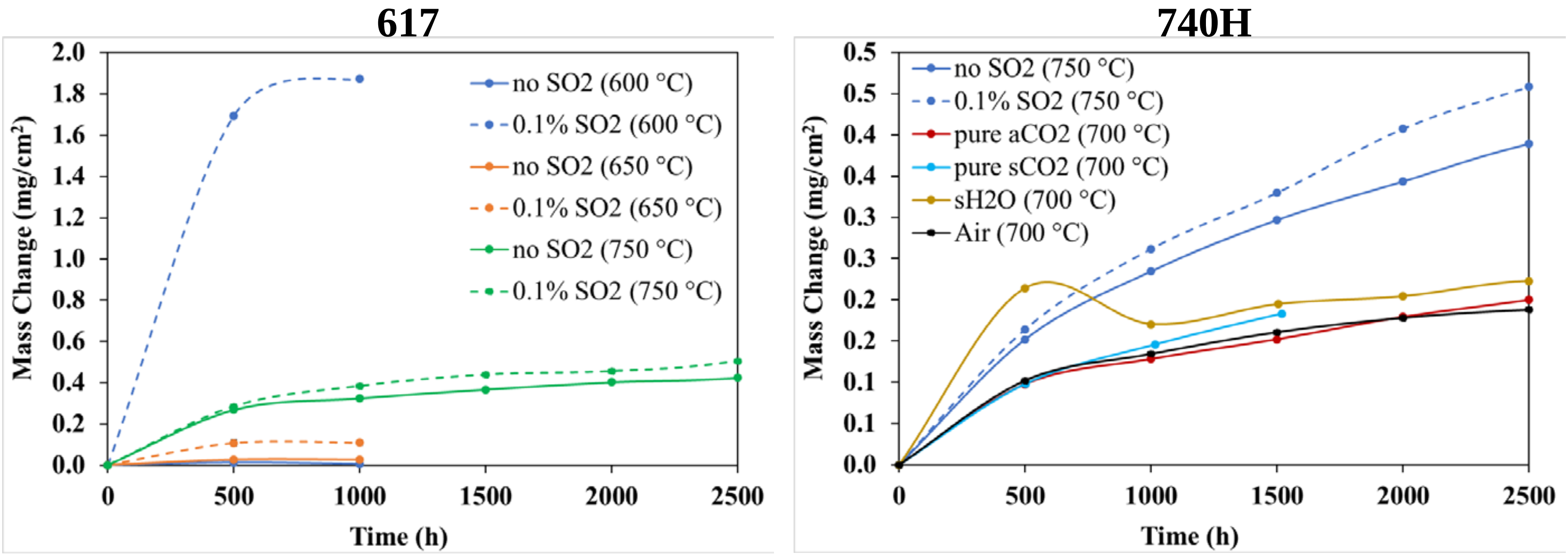

- While there is no negative effect of SO_2 for Ni alloys at 750°C, preliminary results suggest a negative effect that is modest at 650°C & significant at 600°C
- Comparing mass gains in direct-fired environments at 750°C to different environments (pure atmospheric CO_2, pure supercritical CO_2, pure supercritical steam, & air) at similar temperatures shows that the oxidation rates are similar, suggesting minimal effect of impurities at this temperature.

Summary

- Several candidate Fe-based & Ni-based alloys were exposed to 95% CO_2, 4% H_2O, 1% O_2 with/without 0.1% SO_2 at 1 atm & temperatures ranging from 550-750°C to simulate the conditions expected in high temperature portions of a direct-fired sCO_2 power cycle fueled by coal syngas and natural gas, respectively.
- The oxidation performance of Fe alloys was strongly influenced by Cr content, where >11.5 wt% Cr was required to achieve low oxidation rates at temperatures of 550, 600, and 650°C both with/without SO_2. The presence of SO_2 had a negative effect at 550°C & less effect at higher temperatures.
- Ni alloys showed low oxidation rates at 750°C both with/without SO_2 that were comparable to what is seen for other environments (pure CO_2, supercritical steam, etc.). However, preliminary results suggest a strong negative effect of SO_2 at lower temperatures (600°C).
- Microscopic characterization and thermodynamic analysis were used to understand the processes controlling the complex pattern of oxidation behavior for these exposures.